Hindawi
Complexity
Volume 2021, Article ID 6673568, 12 pages
https://doi.org/10.1155/2021/6673568

Research Article

Command Filtering and Barrier Lyapunov Function-Based Adaptive Control for PMSMs with Core Losses and All-State Restrictions

Xiaoling Wang and Jinpeng Yu

College of Automation, Qingdao University, Qingdao 266071, Shandong, China

Correspondence should be addressed to Jinpeng Yu; yjp1109@126.com

Received 26 October 2020; Revised 18 January 2021; Accepted 28 January 2021; Published 10 February 2021

Academic Editor: Xue-bo Jin

With the troubles of core losses and all-state confined to certain limitations which are the innate traits of permanent magnet synchronous motors (PMSMs), this article develops a command filtered adaptive backstepping approach to follow the track of PMSM's desired rotor position. To begin with, the RBF neural network technique is utilized to get close to the uncharted nonlinear terms which existed in PMSM's mathematical model. Meanwhile, an advanced adaptive command filter control methodology is constructed to avoid the computing explosion during the process of backstepping design. Furthermore, to make sure that all the state variables are confined into certain ranges, we employed the barrier Lyapunov function (BLF) at every step of the controllers construction. In addition, an error compensating mechanism is proposed to neutralize filtering errors and only one adaptive law is required. At last, simulation results bear out the superiority of the aforementioned control scheme.

1. Introduction

Lately, permanent magnet synchronous motors (PMSMs) are employed broadly in real-world utilization. This proverbial usage is due to the advantageous PMSMs features like straightforward mechanism, petit size, great productiveness, and dependable manipulation. Nevertheless, the PMSM's real-time mathematic model set contains tremendous nonlinearity and multivariables issues which may lead to a challenging mission to acquire optimum control results. So, in order to enhance the PMSM's control effectiveness, many advanced control techniques have been proposed, for instance, PI control [1, 2], sliding mode control [3–5], adaptive backstepping control [6], and other control schemes [7, 8]. Among these methodologies, the backstepping control technique is now becoming a basic foundation to construct controllers for high complexity models since it was designed to obtain asymptotic tracking and global stability. Besides, the load turbulence and time-variant parameters issues can be ripped out of the operation of PMSMs by making use of the adaptive control technique.

However, "certain functions must be linear" and "explosion of complexity" issues which are rooted in the traditional backstepping control methods are very tricky to be dealt with. For one thing, along with the development of radial basis function (RBF) neural networks (NNs) [9–11], the nonlinear systems' unknown functions can be approximated by this algorithm based on the adaptive control method and this proposal can rule out the dependency of the accurate mathematical model. For another, in [12–14], a command filtered-based backstepping method was developed to tackle the "explosion of complexity" problem and the error compensation technique is employed to make the filtering outcomes more accurate. To be specific, the command filters' input signals are designed as virtual control functions and the filters' outputs can eliminate explosive terms. Moreover, the error compensation mechanism will neutralize the filtering deviations to some extent. But these

published methodologies have not considered the state constraints problem of PMSM drive systems.

In fact, according to the PMSM's inherent features, its state variables should be confined to reasonable boundaries. For instance, if the rotor angular velocity, stator current, or other state variables of PMSM are out of the state constraints, the motor's performance will be influenced and may even result in severe security issues. Take stator current as an example, exorbitant current value will lead to serious overheating problems to the rotators which would speed up the aging of insulation materials and decrease the equipment's service lifespan. Accordingly, state limitations are indispensable during the PMSM's controllers construct process. Fortunately, many significant achievements have been obtained in the all-state constrained nonlinear control field, such as [15, 16] and from these approaches, the barrier Lyapunov functions (BLFs) are normally utilized to hold off the limitation transgressions.

Apart from state variables restrictions, in order to get perfect control performance of PMSMs, the core loss impact also should be taken into consideration when the driving frequency spikes, which is correlated with the high-speed operation. The control accuracy will drop sharply with tremendous core losses, and thus the solution of PMSMs with iron losses problem is crucial to actual applications. As far as we know, the core losses and all-state restrictions issues which are rooted in nonlinear high-ordered PMSM drive systems have not been studied by using command filtered adaptive backstepping approach.

So, with these previous observations, we took core losses and all-state restrictions which are the inherent properties of PMSM drive systems into considerations, and then we developed a BLFs-based adaptive command filtered neural control method. Disparate from the conventional control schemes, this method's main novelties are concluded as follows:

(1) Unlike [17], the command filters are used to tackle the "explosion of complexity" issue which cannot be neglected in adaptive backstepping control for nonlinear systems.

(2) Distinct from [17, 18], this paper considers the core losses issue in PMSM's mathematical model and thus makes this method be more applicable in actual usages.

(3) Different from [12, 19], the errors that arose from command filters are neutralized by compensating signals to diminish their negative influence upon control performance.

(4) This article just requires one single adaptive law during the controllers construction process, which can facilitate the calculation compared to [20], so that the control scheme's effectiveness will be improved.

In the posterior section of this paper, simulation figures and a comparison table are displayed to substantiate the effectiveness and robustness of the submitted control approach.

2. Related Works

2.1. Nonlinear Control Methods. Many approaches are proposed to enhance the control effectiveness of nonlinear systems. In [21], Zheng et al. utilized a stable adaptive PI control strategy in the discrete-time domain for the PMSM drive system. The PI controller is capable of automatic online tuning of the control gains based on the gradient descent method and the experimental results illustrated the tracking performance is favorable. Li et al. [22] put forward the sliding-mode control method to deal with nonlinear active suspension systems. They designed an adaptive sliding-mode controller to guarantee the reachability of the specified switching surface. Yin et al. designed a backstepping controller for the switch complex nonlinear system in [23]. During the construction process, they developed a state backstepping controller to realize the exponential stability of the observer-backstepping feedback control system. Zhang et al. presented a linear quadratic regulator-based proportion integral differential equivalent controller for PMSM in [24]. The method was implemented through the dSPACE digital signal processor system and the experimental result confirmed its effectiveness.

2.2. Approximation Techniques. To enlarge the practical field of the backstepping method, the nonlinear terms in the nonlinear systems' mathematical model need to be dealt with. The literature [25–28] has utilized the fuzzy logic systems (FLS) to approximate unknown nonlinearities in different kinds of scenarios. And the approximation results verified that this technique can well serve its original purpose. In [29–31], the authors employed the LSTM and the GRU techniques to predict traffic speed, power load, and traffic flow, respectively. And the experimental results indicate these two kinds of deep recurrent networks are skilled in modeling abilities, which make them more suitable for sequence-based long-term tasks. In [32], Bai et al. utilized a compound autoregressive network to predict multivariate time series. Jin et al. proposed two nonlinear estimation methods to achieve real-time indoor RFID tracking in [33]. In [9], Fu et al. utilized the RBF neural networks to cope with the unknown nonlinear functions. The finite-time adaptive neural controller was proposed via the new command filter backstepping technique, and the tracking error converges to a small neighborhood of the origin in finite time.

2.3. Filtering Algorithms. Some scholars put forward a variety of filtering methods in recent years. In [34], Bai et al. proposed a neuron-based Kalman filter to enhance the control effect of various intelligent terminals and promote the sensing level. They introduced the neuronunits into the conventional Kalman filter framework and thus the filtering process could be optimized to reduce the effect of the unpractical system model and hypothetical parameters. In [35, 36], the authors employed the dynamic surface control (DSC) technique to resolve the "explosion of complexity" problem, and it is a first-ordered filtering method for every step's virtual input during the traditional backstepping

controllers design. But the DSC technique does not take the deviations ascribed to the first-order filters into account, which may induce unwanted influence on the control result. In [37], the adaptive filtering technique was proposed to filter the complex noise and obtain the true measurements' value and thus the MEMS gyroscope performance can be improved. In [38], the authors proposed a state filtering-based least squares parameter estimation for bilinear systems. Zhang et al. developed a novel state estimation algorithm to enhance the computational efficiency based on delta operator in [39].

2.4. PMSM Innate Features and Identification Methods. In [40, 41], the authors take full-state constraints of nonlinear systems into consideration and constructed the barrier Lyapunov functions to ensure the state constraints are not transgressed. In [42], Zhao et al. proposed a health performance evaluation method to detect anomaly occurrences and evaluate the multirotor system's real-time health condition. Ding et al. in [43, 44] derived gradient-based and two-stage gradient-based iterative algorithms to generate more accurate parameter estimation to overcome the difficulty of state and input identifications. In [45], Zhang et al. developed joint estimation algorithms for states and parameters of nonlinear systems to make the parameter estimates converge to their true values. With the identification methods in [43–45], the parameters of the mathematical models can be obtained accordingly.

3. Dynamic Model and Preparations

In the $d-q$ frame of axes, the PMSM's dynamic model with core losses from [46] can be described as

$$\begin{cases} \dfrac{\mathrm{d}\theta}{\mathrm{d}t} = \omega, \\ \dfrac{\mathrm{d}\omega}{\mathrm{d}t} = \dfrac{n_p\lambda_{PM}}{J} i_{oq} + \dfrac{n_p\left(L_{m\,d} - L_{mq}\right) i_{oq} i_{od}}{J} - \dfrac{T_L}{J}, \\ \dfrac{\mathrm{d}i_{oq}}{\mathrm{d}t} = \dfrac{R_c}{L_{mq}} i_q - \dfrac{R_c}{L_{mq}} i_{oq} - \dfrac{n_p L_d}{L_{mq}} \omega i_{o\,d} - \dfrac{n_p\lambda_{PM}}{L_{mq}}\omega, \\ \dfrac{\mathrm{d}i_q}{\mathrm{d}t} = -\dfrac{R_s}{L_{lq}} i_q + \dfrac{R_c}{L_{lq}} i_{oq} + \dfrac{1}{L_{lq}} u_q, \\ \dfrac{\mathrm{d}i_{o\,d}}{\mathrm{d}t} = \dfrac{R_c}{L_{md}} i_d - \dfrac{R_c}{L_{md}} i_{o\,d} + \dfrac{n_p L_q}{L_{md}} \omega i_{oq}, \\ \dfrac{\mathrm{d}i_d}{\mathrm{d}t} = -\dfrac{R_s}{L_{ld}} i_d + \dfrac{R_c}{L_{ld}} i_{o\,d} + \dfrac{1}{L_{ld}} u_d, \end{cases} \tag{1}$$

where θ, ω, n_p, J, T_L, R_s, and R_c represent rotor position, rotor angular speed, quantity of pole pairs, rotor momental inertia, load torque, stator resistance, and core loss resistance, sequentially. u_d stands for the d-axis voltage and u_q represents the q-axis voltage. i_d is the d-axis current while i_q is the q-axis current. L_d and L_q present as stator inductors. L_{ld} and L_{lq} represent leakage inductances, while L_{md} and L_{mq} are the notations of magnetic inductances. Finally, λ_{PM} stands for the excitation flux. To simplify the above mathematical equations, we employ the following symbolizations:

$$\begin{aligned} x_1 &= \theta, \\ x_2 &= \omega, \\ x_3 &= i_{oq}, \\ x_4 &= i_q, \\ x_5 &= i_{od}, \\ x_6 &= i_d, \\ a_1 &= n_p\lambda_{PM}, \\ a_2 &= n_p\left(L_{md} - L_{mq}\right), \\ b_1 &= \frac{R_c}{L_{mq}}, \\ b_2 &= -\frac{n_p L_d}{L_{mq}}, \\ b_3 &= -\frac{n_p\lambda_{PM}}{L_{mq}}, \\ b_4 &= -\frac{R_s}{L_{lq}}, \\ b_5 &= \frac{R_c}{L_{lq}}, \\ c_1 &= \frac{R_c}{L_{md}}, \\ c_2 &= -\frac{n_p L_q}{L_{md}}, \\ c_3 &= -\frac{R_s}{L_{ld}}, \\ c_4 &= \frac{R_c}{L_{ld}}, \\ d_1 &= \frac{1}{L_{lq}}, \\ d_2 &= \frac{1}{L_{ld}}. \end{aligned} \tag{2}$$

With the aforementioned symbolizations, the mathematical model set will be converted into

$$\begin{aligned}
\dot{x}_1 &= x_2,\\
\dot{x}_2 &= \frac{a_1}{J}x_3 + \frac{a_2}{J}x_3x_5 - \frac{T_L}{J},\\
\dot{x}_3 &= b_1x_4 - b_1x_3 + b_2x_2x_5 + b_3x_2,\\
\dot{x}_4 &= b_4x_4 + b_5x_3 + d_1u_q,\\
\dot{x}_5 &= c_1x_6 - c_1x_5 - c_2x_2x_3,\\
\dot{x}_6 &= c_3x_6 + c_4x_5 + d_2u_d.
\end{aligned} \tag{3}$$

The ultimate goal of this paper is to develop the controllers u_q along with u_d to make the rotor position x_1 track the desired signal x_d as perfect as possible while the state variables x_i are demanded to meet the premises that $|x_i| < k_{c_i}$ $(i = 1, 2, 3, 4, 5, 6)$, in which $k_{c_i} > 0$.

The RBF neural network is a feedforward network with three layers of neurons called the input layer, the hidden layer, and the output layer. Figure 1 is the graphic illustration of the structure of the RBF neural network. Additionally, the input layer contains an equal number of nodes to the dimension of the input vector. The hidden layer's nodes number depends on the complexity of the problem. The output layer's nodes number equals the dimension of the output vector. The weight parameter W stands for the link between nodes and it only exists between the hidden and output layers. The self-training law will be given later. The k-means clustering algorithm which is a kind of unsupervised algorithm of RBF neural network will be used in this paper. With the neural network's theory and its parameters' definitions which can be found in [47], we know that any time-consecutive function $\varphi(z)$ can be estimated by RBF NNs. The estimate functions $\widehat{\varphi}(z) = W^{*T}S(Z)$ satisfy the premise of $R^q \longrightarrow R$, in which q stands for input dimensions. Moreover, the NNs' input variable Z needs to be within the domain of $Z \in \Omega_Z \subset R^q$ and the weight vector W^* is formed as $W^* = [\Phi_1^*, \ldots, \Phi_l^*]^T$, where l represents the quantity of NNs nodes. We choose the Gaussian basis function $S(Z) = ([p_1(Z), p_2(Z), \ldots, p_n(Z)]^T / \sum_{i=1}^{n} p_i(Z))$ and $p_i(Z) = \exp[(-(Z-\eta_i)^T(Z-\eta_i))/\gamma_i^2]$ for $i = 1, 2, \ldots, n$, where $\eta_i = [\eta_{i1}, \eta_{i2}, \ldots, \eta_{in}]^T$ is the center vector and γ_i is the Gaussian function's width. So, with the above definitions, the inequality $\|W_i(S_i(k))\|^2 \le l_i$ $(i = 1, \ldots, n)$ holds.

Lemma 1 *From* [12], we have the definition of command filters listed as

$$\begin{aligned}
\dot{e}_1 &= \omega_n e_2,\\
\dot{e}_2 &= -2\xi\omega_n e_2 - \omega_n(e_1 - \alpha_1).
\end{aligned} \tag{4}$$

From the above equations, we know that the output variables e_1 and e_2 can be obtained by the input variable α_1. In order to do so, there are some rules that should be satisfied. Firstly, for all $t \ge 0$, the first and second ordered time derivative forms of α_1 should meet the demands of $|\dot{\alpha}_1| < \rho_1$ and $|\ddot{\alpha}_1| < \rho_2$ while ρ_1, ρ_2 are positive constants. Secondly, the initial conditions of these variables should satisfy that $e_1(0) = \alpha_1(0)$, $e_2(0) = 0$. Consequently, $|\dot{e}_1|$, $|\ddot{e}_1|$, and $|\dddot{e}_1|$ will be bounded into certain ranges. Additionally, with $\xi \in (0, 1]$ and $\omega_n > 0$, the deviation between the input and output signals will satisfy that $|e_1 - \alpha_1| \le \mu$.

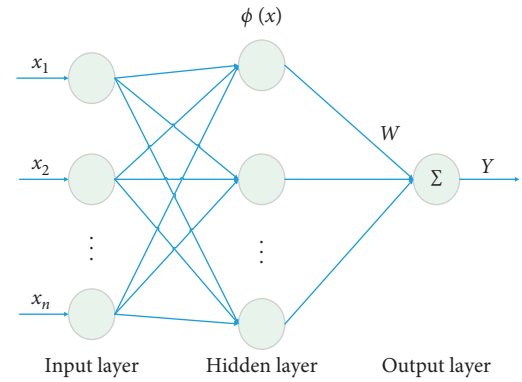

Figure 1: The structure of RBF neural network.

Assumption 1 (see [41]). The desired signal x_d and its first-ordered time derivative form $\dot{x}_d$ should both be smooth, limited, and known. Thus, they can meet the demands of $|x_d| \le Y_0 < k_{c_1}$ and $|\dot{x}_d| \le Y_1$, in which Y_0 and Y_1 are positive constants.

4. Command Filtered Self-Adaptive Neural Network Controllers Construction

During this process, we constructed the self-adaptive command filtered neural network controllers for PMSMs with core losses and all-state restrictions based on the BLFs. To begin with, we define the error variables as

$$\begin{aligned}
z_1 &= x_1 - x_d,\\
z_2 &= x_2 - x_{1,c},\\
z_3 &= x_3 - x_{2,c},\\
z_4 &= x_4 - x_{3,c},\\
z_5 &= x_5,\\
z_6 &= x_6 - x_{4,c},\\
v_1 &= z_1 - \zeta_1,\\
v_2 &= z_2 - \zeta_2,\\
v_3 &= z_3 - \zeta_3,\\
v_4 &= z_4 - \zeta_4,\\
v_5 &= z_5 - \zeta_5,\\
v_6 &= z_6 - \zeta_6,
\end{aligned} \tag{5}$$

where x_d is the desired rotor position trajectory and α_i are the input variables of the filters while $x_{i,c}$ represent the filters' output variables, in which $i = 1, 2, 3, 4$. To neutralize the filtering errors which are the values of $x_{i,c} - \alpha_i$, at every filtering step, we use the error compensation technique and ζ_i represent the compensation signals, where $i = 1, 2, 3, 4, 5, 6$. Additionally, we introduce a tight set

$\Omega_v = \{|v_i| < k_{b_i}, i = 1, 2, \ldots, 6\}$, in which the constants k_{b_i} should be positive. During the next construction process, the error renumeration variables ζ_i, the virtual controllers α_i, and the real controllers u_d and u_q will be given.

Step 1. In [15], the barrier Lyapunov function was proposed. So, with the description, we select the first BLF V_1 as

$$V_1 = \frac{1}{2}\log\left(\frac{k_{b_1}^2}{k_{b_1}^2 - v_1^2}\right). \tag{6}$$

Within the compact set Ω_v, the first-ordered time derivative form of V_1 should be

$$\dot{V}_1 = K_{v_1}\dot{v}_1 = K_{v_1}\left(z_2 + x_{1,c} - \dot{x}_d - \dot{\zeta}_1\right), \tag{7}$$

in which $K_{v_i} = (v_i/(k_{b_i}^2 - v_i^2))$, $i = 1, 2, \ldots, 6$. Next, we conceive the virtual controller α_1 and the remunerate variable ζ_1 as

$$\begin{aligned} \alpha_1 &= -k_1 z_1 + \dot{x}_d, \\ \dot{\zeta}_1 &= -k_1\zeta_1 + \zeta_2 + \left(x_{1,c} - \alpha_1\right), \end{aligned} \tag{8}$$

where $k_1 > 0$ is designed to be the control gain and the terms $k_i > 0$ $(i = 1, 2, \ldots, 6)$ will be applied in constructing other virtual control laws and compensation signals later on. By using (8), (7) can be converted into the following equation:

$$\dot{V}_1 = -k_1 K_{v_1} v_1 + K_{v_1} v_2. \tag{9}$$

Step 2. Similarly, we set up the second BLF as

$$V_2 = V_1 + \frac{J}{2}\log\left(\frac{k_{b_2}^2}{k_{b_2}^2 - v_2^2}\right), \tag{10}$$

where V_2 should be time-consecutive within the compact set Ω_v, so we compute its first-ordered time derivative form and apply $\dot{V}_1$ into it to get the following equation:

$$\begin{aligned} \dot{V}_2 &= \dot{V}_1 + JK_{v_2}\dot{v}_2 \\ &= -k_1 K_{v_1} v_1 + K_{v_1} v_2 + K_{v_2}\left(a_1 x_3 + a_2 x_3 x_5 - T_L - J\dot{x}_{1,c} - J\dot{\zeta}_2\right). \end{aligned} \tag{11}$$

When it comes to actual applications, T_L is presumed to be unknown but should be limited to a certain range. Therefore, we assume $|T_L| \le d$, in which the constant d should be positive. With Young's inequality theorem, we have $-K_{v_2}T_L \le (1/2\varepsilon_1^2)K_{v_2}^2 + (1/2)\varepsilon_1^2 d^2$ with $\varepsilon_1 > 0$.

So, rewritten $\dot{V}_2$ as

$$\dot{V}_2 \le -k_1 K_{v_1} v_1 + K_{v_1} v_2 + K_{v_2}\left(a_1 x_3 - J\dot{\zeta}_2 + f_2(Z)\right) + \frac{1}{2}\varepsilon_1^2 d^2, \tag{12}$$

in which $f_2(Z) = a_2 x_3 x_5 - J\dot{x}_{1,c} + (1/2\varepsilon_1^2)K_{v_2}$, $Z = [x_1, x_2, x_3, x_4, x_5, x_6, x_d, \dot{x}_d]^T$. With the aforementioned description of RBF NNs, we know that it always has a RBF NN $W_2^T S_2(Z)$ to make $f_2(Z) = W_2^T S_2(Z) + \delta_2(Z)$ holds, where $\delta_2(Z)$ is the estimate error. Then, for any $\varepsilon_2 > 0$, $\delta_2(Z)$ will satisfy that $|\delta_2(Z)| \le \varepsilon_2$. So, under the premise of $l_2 > 0$, we have

$$\begin{aligned} K_{v_2} f_2(Z) &= K_{v_2}\left(W_2^T S_2(Z) + \delta_2(Z)\right) \\ &\le \frac{\|W_2\|^2 K_{v_2}^2 S_2^T S_2}{2l_2^2} + \frac{l_2^2}{2} + \frac{K_{v_2}^2}{2} + \frac{\varepsilon_2^2}{2}. \end{aligned} \tag{13}$$

Design the second virtual control signal α_2 along with the remuneration variable ζ_2 as

$$\begin{aligned} \alpha_2 &= -\frac{1}{a_1}\left(k_2 z_2 + \frac{K_{v_2}}{2} + \frac{K_{v_2}\widehat{\theta} S_2^T S_2}{2l_2^2} + K_{v_1}\left(k_{b_2}^2 - v_2^2\right)\right), \\ \dot{\zeta}_2 &= -\frac{1}{J}\left(k_2\zeta_2 - a_1\zeta_3 - a_1\left(x_{2,c} - \alpha_2\right)\right), \end{aligned} \tag{14}$$

with $\widehat{\theta}$ being the approximation of θ, which will be constructed later on. Applying (13) and (14) into (12), we have

$$\begin{aligned} \dot{V}_2 \le & -k_1 K_{v_1} v_1 - k_2 K_{v_2} v_2 + K_{v_2} a_1 v_3 + \frac{1}{2}\varepsilon_1^2 d^2 \\ & + \frac{\left(\|W_2\|^2 - \widehat{\theta}\right)K_{v_2}^2 S_2^T S_2}{2l_2^2} + \frac{l_2^2}{2} + \frac{\varepsilon_2^2}{2}. \end{aligned} \tag{15}$$

Step 3. Construct the third BLF as

$$V_3 = V_2 + \frac{1}{2}\log\left(\frac{k_{b_3}^2}{k_{b_3}^2 - v_3^2}\right), \tag{16}$$

V_3 is continuous within the compact set Ω_v, so we compute its first-ordered time derivative form and apply $\dot{V}_2$ into it, then we get

$$\begin{aligned} \dot{V}_3 \le & -\sum_{i=1}^{2} k_i K_{v_i} v_i + K_{v_2} a_1 v_3 + K_{v_3}\left(b_1 x_4 - \dot{x}_{2,c} - \dot{\zeta}_3 + f_3(Z)\right) \\ & + \frac{\left(\|W_2\|^2 - \widehat{\theta}\right)K_{v_2}^2 S_2^T S_2}{2l_2^2} + \frac{l_2^2}{2} + \frac{\varepsilon_2^2}{2} + \frac{1}{2}\varepsilon_1^2 d^2, \end{aligned} \tag{17}$$

in which $f_3(Z) = -b_1 x_3 + b_2 x_2 x_5 + b_3 x_2$. Akin to Step 2, it always has a RBF NN $W_3^T S_3(Z)$ to make $f_3(Z) = W_3^T S_3(Z) + \delta_3(Z)$ holds, where $\delta_3(Z)$ is the estimate error. Then, for any $\varepsilon_3 > 0$, $\delta_3(Z)$ will satisfy that $|\delta_3(Z)| \le \varepsilon_3$. With the premise of $l_3 > 0$, we deduce that

$$\begin{aligned} K_{v_3} f_3(Z) &= K_{v_3}\left(W_3^T S_3(Z) + \delta_3(Z)\right) \\ &\le \frac{\|W_3\|^2 K_{v_3}^2 S_3^T S_3}{2l_3^2} + \frac{l_3^2}{2} + \frac{K_{v_3}^2}{2} + \frac{\varepsilon_3^2}{2}. \end{aligned} \tag{18}$$

Set the third virtual control law α_3 along with the remuneration variable ζ_3 as

$$\alpha_3 = -\frac{1}{b_1}\left(k_3 z_3 + \frac{K_{v_3}}{2} + \frac{K_{v_3}\widehat{\theta}S_3^T S_3}{2l_3^2} + a_1 K_{v_2}\left(k_{b_3}^2 - v_3^2\right) - \dot{x}_{2,c}\right),$$
$$\dot{\zeta}_3 = -k_3\zeta_3 + b_1\zeta_4 + b_1\left(x_{3,c} - \alpha_3\right). \tag{19}$$

Applying (18) and (19) into (17), we have

$$\dot{V}_3 \le -\sum_{i=1}^{3} k_i K_{v_i} v_i + b_1 K_{v_3} v_4 + \sum_{i=2}^{3}\frac{\left(\|W_i\|^2 - \widehat{\theta}\right)K_{v_i}^2 S_i^T S_i}{2l_i^2} + \sum_{i=2}^{3}\frac{l_i^2}{2} + \sum_{i=2}^{3}\frac{\varepsilon_i^2}{2} + \frac{1}{2}\varepsilon_1^2 d^2. \tag{20}$$

Step 4. Design the next BLF V_4 as

$$V_4 = V_3 + \frac{1}{2}\log\left(\frac{k_{b_4}^2}{k_{b_4}^2 - v_4^2}\right). \tag{21}$$

Akin to $\dot{V}_3$, $\dot{V}_4$ will be listed as

$$\dot{V}_4 \le -\sum_{i=1}^{3} k_i K_{v_i} v_i + b_1 K_{v_3} v_4 + K_{v_4}\left(d_1 u_q - \dot{x}_{3,c} - \dot{\zeta}_4 + f_4(Z)\right) + \sum_{i=2}^{3}\frac{\left(\|W_i\|^2 - \widehat{\theta}\right)K_{v_i}^2 S_i^T S_i}{2l_i^2} + \sum_{i=2}^{3}\frac{l_i^2}{2} + \sum_{i=2}^{3}\frac{\varepsilon_i^2}{2} + \frac{1}{2}\varepsilon_1^2 d^2, \tag{22}$$

in which $f_4(Z) = b_4 x_4 + b_5 x_3$. Akin to the last step, it always has a neural network $W_4^T S_4(Z)$ to make that $f_4(Z) = W_4^T S_4(Z) + \delta_4(Z)$ holds, where $\delta_4(Z)$ stands for the estimate error. Then, for any $\varepsilon_4 > 0$, $\delta_4(Z)$ will satisfy that $|\delta_4(Z)| \le \varepsilon_4$. So, with the premise of $l_4 > 0$, we can obtain that

$$K_{v_4} f_4(Z) = K_{v_4}\left(W_4^T S_4(Z) + \delta_4(Z)\right) \le \frac{\|W_4\|^2 K_{v_4}^2 S_4^T S_4}{2l_4^2} + \frac{l_4^2}{2} + \frac{K_{v_4}^2}{2} + \frac{\varepsilon_4^2}{2}. \tag{23}$$

Now, we set the actual control signal u_q and the remunerate variable ζ_4 as

$$u_q = -\frac{1}{d_1}\left(k_4 z_4 + \frac{1}{2}K_{v_4} + \frac{K_{v_4}\widehat{\theta}S_4^T S_4}{2l_4^2} + b_1 K_{v_3}\left(k_{b_4}^2 - v_4^2\right) - \dot{x}_{3,c}\right),$$
$$\dot{\zeta}_4 = -k_4\zeta_4. \tag{24}$$

Then, with the terms of (23) and (24), the inequality (22) will result in

$$\dot{V}_4 \le -\sum_{i=1}^{4} k_i K_{v_i} v_i + \sum_{i=2}^{4}\frac{\left(\|W_i\|^2 - \widehat{\theta}\right)K_{v_i}^2 S_i^T S_i}{2l_i^2} + \sum_{i=2}^{4}\frac{l_i^2}{2} + \sum_{i=2}^{4}\frac{\varepsilon_i^2}{2} + \frac{1}{2}\varepsilon_1^2 d^2. \tag{25}$$

Step 5. Set the next BLF V_5 as

$$V_5 = V_4 + \frac{1}{2}\log\left(\frac{k_{b_5}^2}{k_{b_5}^2 - v_5^2}\right), \tag{26}$$

where V_5 is continuous within the compact set Ω_v, so we compute its first-ordered time derivative form and apply $\dot{V}_4$ into it; then, we have

$$\dot{V}_5 \le -\sum_{i=1}^{4} k_i K_{v_i} v_i + K_{v_5}\left(c_1 x_6 - \dot{\zeta}_5 + f_5(Z)\right) + \sum_{i=2}^{4}\frac{\left(\|W_i\|^2 - \widehat{\theta}\right)K_{v_i}^2 S_i^T S_i}{2l_i^2} + \sum_{i=2}^{4}\frac{l_i^2}{2} + \sum_{i=2}^{4}\frac{\varepsilon_i^2}{2} + \frac{1}{2}\varepsilon_1^2 d^2, \tag{27}$$

in which $f_5(Z) = -c_1 x_5 - c_2 x_2 x_3 = W_5^T S_5(Z) + \delta_5(Z)$, $|\delta_5(Z)| \le \varepsilon_5$. With the premise of $l_5 > 0$, we can deduce that

$$K_{v_5} f_5(Z) = K_{v_5}\left(W_5^T S_5(Z) + \delta_5(Z)\right) \le \frac{\|W_5\|^2 K_{v_5}^2 S_5^T S_5}{2l_5^2} + \frac{l_5^2}{2} + \frac{K_{v_5}^2}{2} + \frac{\varepsilon_5^2}{2}. \tag{28}$$

Design the fourth virtual control signal α_4 along with the remunerate variable ζ_5 as

$$\alpha_4 = -\frac{1}{c_1}\left(k_5 z_5 + \frac{K_{v_5}}{2} + \frac{K_{v_5}\widehat{\theta}S_5^T S_5}{2l_5^2}\right),$$
$$\dot{\zeta}_5 = -k_5\zeta_5 + c_1\zeta_6 + c_1\left(x_{4,c} - \alpha_4\right). \tag{29}$$

By using (28) and (29), inequality (27) can be transformed as

$$\dot{V}_5 \le -\sum_{i=1}^{5} k_i K_{v_i} v_i + c_1 K_{v_5} v_6 + \sum_{i=2}^{5}\frac{\left(\|W_i\|^2 - \widehat{\theta}\right)K_{v_i}^2 S_i^T S_i}{2l_i^2} + \sum_{i=2}^{5}\frac{l_i^2}{2} + \sum_{i=2}^{5}\frac{\varepsilon_i^2}{2} + \frac{1}{2}\varepsilon_1^2 d^2. \tag{30}$$

Step 6. Design the sixth BLF V_6 as follows:

$$V_6 = V_5 + \frac{1}{2}\log\left(\frac{k_{b_6}^2}{k_{b_6}^2 - v_6^2}\right). \tag{31}$$

Similarly,

$$\dot{V}_6 \le -\sum_{i=1}^{5} k_i K_{v_i} v_i + c_1 K_{v_5} v_6 + K_{v_6}\left(d_2 u_d - \dot{x}_{4,c} - \dot{\zeta}_6 + f_6(Z)\right) + \sum_{i=2}^{5} \frac{\left(\|W_i\|^2 - \widehat{\theta}\right) K_{v_i}^2 S_i^T S_i}{2l_i^2} + \sum_{i=2}^{5} \frac{l_i^2}{2} + \sum_{i=2}^{5} \frac{\varepsilon_i^2}{2} + \frac{1}{2}\varepsilon_1^2 d^2. \tag{32}$$

in which $f_6(Z) = c_3 x_6 + c_4 x_5 = W_6^T S_6(Z) + \delta_6(Z)$, $|\delta_6(Z)| \le \varepsilon_6$. With the premise of $l_6 > 0$, we have

$$K_{v_6} f_6(Z) = K_{v_6}\left(W_6^T S_6(Z) + \delta_6(Z)\right) \le \frac{\|W_6\|^2 K_{v_6}^2 S_6^T S_6}{2l_6^2} + \frac{l_6^2}{2} + \frac{K_{v_6}^2}{2} + \frac{\varepsilon_6^2}{2}. \tag{33}$$

Another actual control law u_d along with the remunerate variable ζ_6 will be constructed as

$$u_d = -\frac{1}{d_2}\left(k_6 z_6 + \frac{1}{2}K_{v_6} + \frac{K_{v_6}\widehat{\theta} S_6^T S_6}{2l_6^2} + c_1 K_{v_5}\left(k_{b_6}^2 - v_6^2\right) - \dot{x}_{4,c}\right),$$
$$\dot{\zeta}_6 = -k_6 \zeta_6. \tag{34}$$

Substituting (33) and (34) into (32), we get

$$\dot{V}_6 \le -\sum_{i=1}^{6} k_i K_{v_i} v_i + \sum_{i=2}^{6} \frac{(\theta - \widehat{\theta}) K_{v_i}^2 S_i^T S_i}{2l_i^2} + \sum_{i=2}^{6}\left(\frac{l_i^2}{2} + \frac{\varepsilon_i^2}{2}\right) + \frac{1}{2}\varepsilon_1^2 d^2, \tag{35}$$

where $\theta = \max\left\{\|W_2\|^2, \|W_3\|^2, \|W_4\|^2, \|W_5\|^2, \|W_6\|^2\right\}$ and $\widetilde{\theta} = \widehat{\theta} - \theta$. Define the final BLF as

$$V = V_6 + \frac{1}{2r}\widetilde{\theta}^2. \tag{36}$$

Then, we compute the V's first-ordered time derivative form as

$$\dot{V} \le -\sum_{i=1}^{6} k_i K_{v_i} v_i + \sum_{i=2}^{6}\left(\frac{l_i^2}{2} + \frac{\varepsilon_i^2}{2}\right) + \frac{1}{r}\widetilde{\theta}\left(-\sum_{i=2}^{6} \frac{r K_{v_i}^2 S_i^T S_i}{2l_i^2} + \dot{\widehat{\theta}}\right) + \frac{1}{2}\varepsilon_1^2 d^2. \tag{37}$$

From (37), we choose the self-adaptive signal (also serve as self-training law) $\widehat{\theta}$ as

$$\dot{\widehat{\theta}} = \sum_{i=2}^{6} \frac{r K_{v_i}^2 S_i^T S_i}{2l_i^2} - m\widehat{\theta}, \tag{38}$$

in which the constants m and r should be positive.

Theorem 1. *From this aforementioned design process, we have proposed the real controllers (u_q and u_d), the self-adaptive signal $\widehat{\theta}$, and the remunerate variables ($\zeta_i, i = 1, 2, 3, 4, 5, 6$), and thus, with the PMSM driving systems satisfying Assumption 1 in set Ω_v, by selecting reasonable system parameters and by guaranteeing all-state variables within limitations, we can verify that the tracking errors would be bounded into a small range of origin.*

Proof. The detailed proof will be elaborated in the next section. □

5. Stability Analysis

To illustrate the system's constancy, replacing (38) into (37),

$$\dot{V} \le -\sum_{i=1}^{6} k_i K_{v_i} v_i + \sum_{i=2}^{6}\left(\frac{l_i^2}{2} + \frac{\varepsilon_i^2}{2}\right) + \frac{1}{2}\varepsilon_1^2 d^2 - \frac{m\widetilde{\theta}\widehat{\theta}}{r}. \tag{39}$$

It has been verified that $\log k_{b_i}^2/(k_{b_i}^2 - v_i^2) < (v_i^2/(k_{b_i}^2 - v_i^2))$ in the set $|v_i| < k_{b_i}$ in [48]. Plus, by using $-\widetilde{\theta}\widehat{\theta} \le -(\widetilde{\theta}^2/2) + (\theta^2/2)$, the inequality (39) will be converted into

$$\dot{V} \le -\sum_{i=1}^{6} k_i \log\left(\frac{k_{b_i}^2}{k_{b_i}^2 - v_i^2}\right) - \frac{m\widetilde{\theta}^2}{2r} + \sum_{i=2}^{6}\left(\frac{l_i^2}{2} + \frac{\varepsilon_i^2}{2}\right) + \frac{1}{2}\varepsilon_1^2 d^2 + \frac{m\theta^2}{2r} \le -aV + b, \tag{40}$$

in which $a = \min\{2k_1, (2k_2/J), 2k_3, 2k_4, 2k_5, 2k_6, m\}$ and $b = \sum_{i=2}^{6}((l_i^2/2) + \varepsilon_i^2/2) + (1/2)\varepsilon_1^2 d^2 + (m\theta^2/2r)$. With (40), we can infer that $(\log k_{b_i}^2/(k_{b_i}^2 - v_i^2))$ and $\widetilde{\theta}$ will be all inside of the confined bounds. For inequality (40), multiplying e^{at} at both sides, we have $(\mathrm{d}(V(t)e^{at})/(\mathrm{d}t) \le be^{at})$. Next, at the time range of $[0, t]$, we integrate this inequality and then it can be transformed into

$$V(t) \le \left(V(0) - \frac{b}{a}\right)e^{-at} + \frac{b}{a} \le V(0) + \frac{b}{a}. \tag{41}$$

From inequality (41), we have $|v_i| < k_{b_i}$ and $\widetilde{\theta}$ will be all limited to certain bounds. Moreover, we can infer that $\lim_{t\longrightarrow\infty}(\log(k_{b_i}^2/(k_{b_i}^2 - v_i^2))) \le (2b/a)$ and $\lim_{t\longrightarrow\infty}|v_1| \le k_{b_1}\sqrt{1 - e^{-(2b/a)}}$.

Remark 1. For compensating signals, we set the Lyapunov function as

$$V_0 = \frac{1}{2}\zeta_1^2 + \frac{J}{2}\zeta_2^2 + \frac{1}{2}\zeta_3^2 + \frac{1}{2}\zeta_4^2 + \frac{1}{2}\zeta_5^2 + \frac{1}{2}\zeta_6^2. \tag{42}$$

By employing Lemma 1, we can obtain

$$\begin{aligned}\dot{V}_0 &= \zeta_1\dot{\zeta}_1 + J\zeta_2\dot{\zeta}_2 + \zeta_3\dot{\zeta}_3 + \zeta_4\dot{\zeta}_4 + \zeta_5\dot{\zeta}_5 + \zeta_6\dot{\zeta}_6 \\ &\le -k_1\zeta_1^2 + \zeta_1\zeta_2 + |\zeta_1|\mu - k_2\zeta_2^2 + a_1\zeta_2\zeta_3 + a_1|\zeta_2|\mu - k_3\zeta_3^2 \\ &\quad + b_1\zeta_3\zeta_4 + b_1|\zeta_3|\mu - k_4\zeta_4^2 - k_5\zeta_5^2 + c_1\zeta_5\zeta_6 \\ &\quad + c_1|\zeta_5|\mu - k_6\zeta_6^2 \\ &\le -(k_1-1)\zeta_1^2 - \left(k_2 - \frac{1}{2} - a_1\right)\zeta_2^2 - \left(k_3 - \frac{a_1}{2} - b_1\right)\zeta_3^2 \\ &\quad - \left(k_4 - \frac{b_1}{2}\right)\zeta_4^2 - (k_5 - c_1)\zeta_5^2 - \left(k_6 - \frac{c_1}{2}\right)\zeta_6^2 \\ &\quad + \frac{1 + a_1 + b_1 + c_1}{2}\mu^2 \\ &\le -a_0V_0 + b_0.\end{aligned} \tag{43}$$

in which $a_0 = \min\{2(k_1 - 1), (2/J)(k_2 - (1/2) - a_1), 2(k_3 - (a_1/2) - b_1), 2(k_4 - (b_1/2)), 2(k_5 - c_1), 2(k_6 - (c_1/2))\}$, and $b_0 = ((1 + a_1 + b_1 + c_1)/2)\mu^2$. Therefore, with these two equations, we have

$$\lim_{t\longrightarrow\infty}|\zeta_i| \le \sqrt{\frac{1 + a_1 + b_1 + c_1}{a_0}}\mu, \tag{44}$$

where $i = 1, 2, \ldots, 6$. Since $\nu_1 = z_1 - \zeta_1$, we can infer that $|z_1| \le |\nu_1| + |\zeta_1| < k_{b_1}\sqrt{1 - e^{-(2b/a)}} + \sqrt{((1 + a_1 + b_1 + c_1)/a_0)}\mu$.

Remark 2. Ensue from the definition of a and b, along with the proper control variables m and $k_i\,(i = 1, 2, \ldots, 6)$, small variables $\varepsilon_j\,(j = 2, 3, \ldots, 6)$, $l_n\,(n = 2, 3, \ldots, 6)$, and large parameter r, the rotor position tracking error $|z_1|$ will be small enough to meet the control requirement. On account of $z_1 = x_1 - x_d$ as well as $x_d \le Y_0$, we have $|x_1| < k_{b_1} + \sqrt{((1 + a_1 + b_1 + c_1)/a_0)}\mu + Y_0 \le k_{c_1}$. With the definition of α_1 in equation (8), we know that α_1 contains the terms of z_1 as well as $\dot{x}_d$. Therefore, the upper limitation of α_1 which is noted as ι_1 holds. From $|x_{1,c} - \alpha_1| \le \mu$, we have $|x_{1,c}| \le \mu + \iota_1 \le \lambda_1$. Additionally, with $\nu_2 = z_2 - \zeta_2$, we get $|z_2| \le |\nu_2| + |\zeta_2| < k_{b_2} + \sqrt{((1 + a_1 + b_1 + c_1)/a_0)}\mu$. So, with $z_2 = x_2 - x_{1,c}$, it is obvious that $|x_2| \le |z_2| + |x_{1,c}| < k_{c_2}$. Parallelly, it can be verified that $|x_3| < k_{c_3}$, $|x_4| < k_{c_4}$, $|x_5| < k_{c_5}$, and $|x_6| < k_{c_6}$. At this point, the proof is accomplished.

6. Simulation Results

To substantiate the control scheme's validity, a simulation has been conducted in this part. The PMSM's parameters with core losses are chosen as Table 1.

We set all-state variables' original conditions to zero and choose $x_d = 0.5\sin(t) + 0.5\sin(0.5t)$ as the desired signal. So, $\theta = \max\{\|W_2\|^2, \|W_3\|^2, \|W_4\|^2, \|W_5\|^2, \|W_6\|^2\} = 0$. Moreover, the limitations of PMSM's state variables are $|x_1| \le 2$, $|x_2| \le 15$, $|x_3| \le 30, |x_4| \le 30, |x_5| \le 15, |x_6| \le 20$.

Table 1: Parameters of PMSM with core losses.

$L_d = 0.00977$ H	$L_{md} = 0.007$ H	$\lambda_{PM} = 0.0844$ Wb
$L_q = 0.00977$ H	$L_{mq} = 0.008$ H	$J = 0.002$ Kg · m^2
$L_{ld} = 0.00177$ H	$R_s = 2.21\,\Omega$	$n_p = 3$
$L_{lq} = 0.00177$ H	$R_c = 200\,\Omega$	

Additionally, we selected the load toque as $T_L = \begin{cases} 1, 0 \le t < 15 \\ 1.5, t \ge 15 \end{cases}$. All these parameters of PMSM are obtained based on former experiences in [17, 20, 24]. Certainly, they can be obtained by some identification methods, such as gradient estimation algorithms [43], two-stage gradient-based iterative estimation method [44], or recursive parameter estimation methods [45].

As to the RBF neural network, the neurons' quantity is 11 and we choose the activate functions as $S(x) = ([p_2(x), p_3(x), \ldots, p_6(x)]^T / \sum_{i=2}^{6} p_i(x))$ and $p_i(x) = \exp[((-(x - \eta_i)^T(Z - \eta_i))/\gamma_i^2)]$ for $i = 2, 3, 4, 5, 6$. The activate functions' centers are scattered evenly in scale $[-5, 5]$, and their widths are all defined as 1.

(a) To control the PMSM driving system with core losses and all-state restrictions, we developed the BLFs-based adaptive command filtered neural network controllers. So, during this simulation, we employed control coefficients as $k_1 = 10$, $k_2 = 7$, $k_3 = 100$, $k_4 = 50$, $k_5 = 20$, $k_6 = 30$, $r = 0.05$, $m = 0.02$, $l_2 = l_3 = l_4 = l_5 = l_6 = 0.25$, $k_{b_1} = 1$, $k_{b_2} = 10$, $k_{b_3} = 20$, $k_{b_4} = 20$, $k_{b_5} = 10$, $k_{b_6} = 15$, $\xi = 0.9$, and $\omega_n = 2000$.

(b) To show the superiority of the introduced methodology in this article, we also established the dynamic surface adaptive neural network controllers to control this system. To be comparable, we utilized identically the same parameters which are displayed in (a).

Next, Figures 2–7 illustrate these two simulations outcomes, in which Figures 2(a)–7(a) display the BLFs-based command filtered control (CFC) approach which was introduced in the frontal part of this article, while Figures 2(b)–7(b) demonstrate the dynamic surface control (DSC) scheme under the same circumstance. Figure 2 simulate the curves of x_1 and x_d. Figure 3 display the tracking error z_1. Figures 4 and 5 are the curves of u_q and u_d, respectively. Figures 6 and 7 are the performances of state variables x_2, x_3, x_4, x_5, and x_6.

From these simulation outcomes, we can observe that even under load torque uncertainty, these two approaches can both follow the given trajectory nicely. But it cannot be ignored that the tracking error which is showed in Figure 3(a) is much smaller than the error that was displayed in Figure 3(b). Moreover, the state variables in Figures 6(a) and 7(a) are controlled in the confined ranges, but i_{oq} of Figure 6(b) is varying from −20 to 60, which overstepped the presupposed current's constraint (Table 2).

Remark 3. Disparate from the DSC control method without taking filtering errors into consideration, in this paper, we

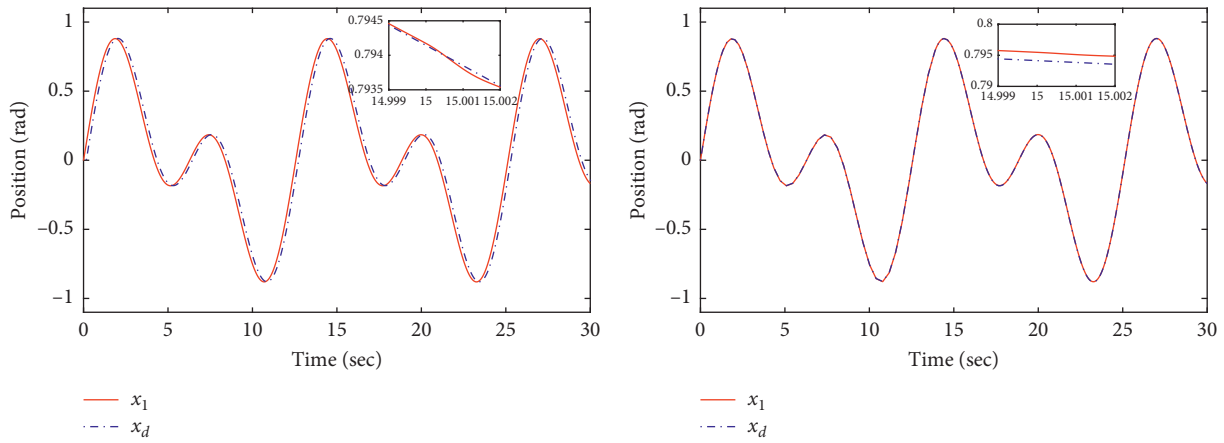

Figure 2: (a) x_1 and x_d for BLFs-based CFC. (b) x_1 and x_d for DSC.

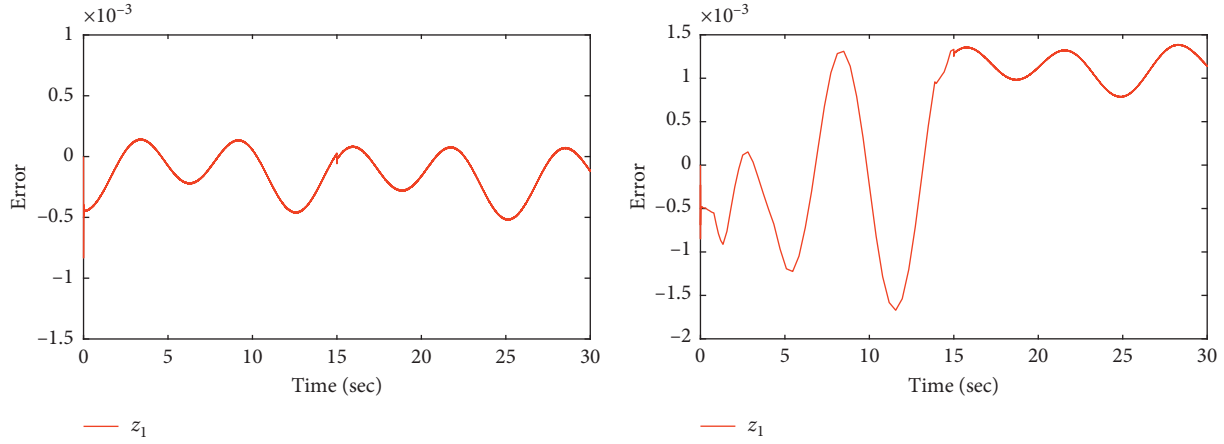

Figure 3: (a) Tracking error for BLFs-based CFC. (b) Tracking error for DSC.

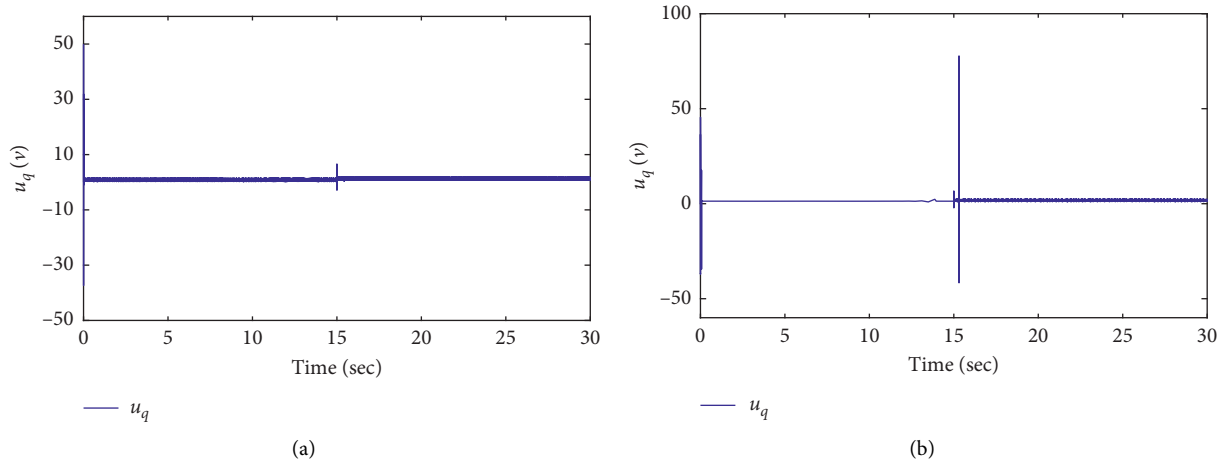

Figure 4: (a) u_q for BLFs-based CFC. (b) u_q for DSC.

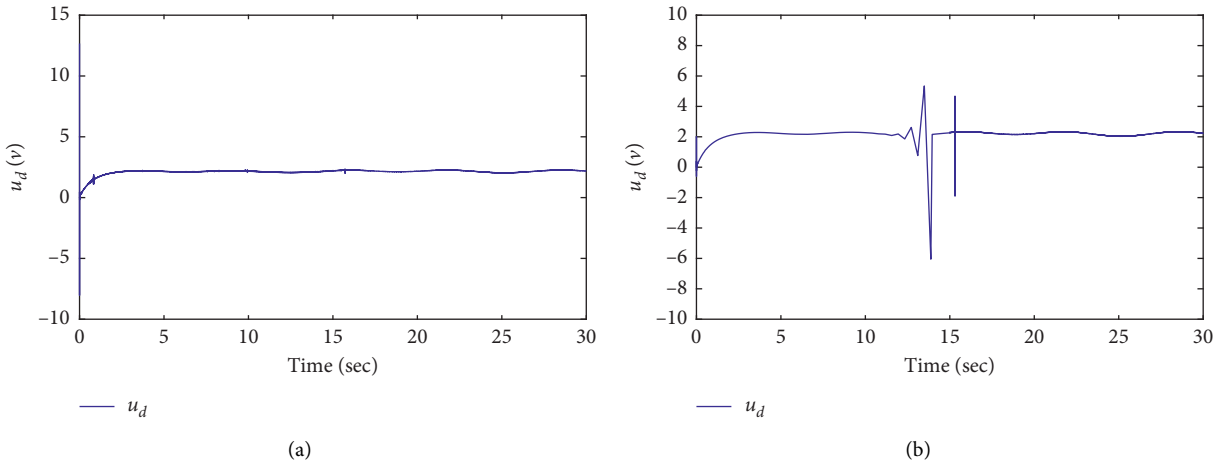

Figure 5: (a) u_d for BLFs-based CFC. (b) u_d for DSC.

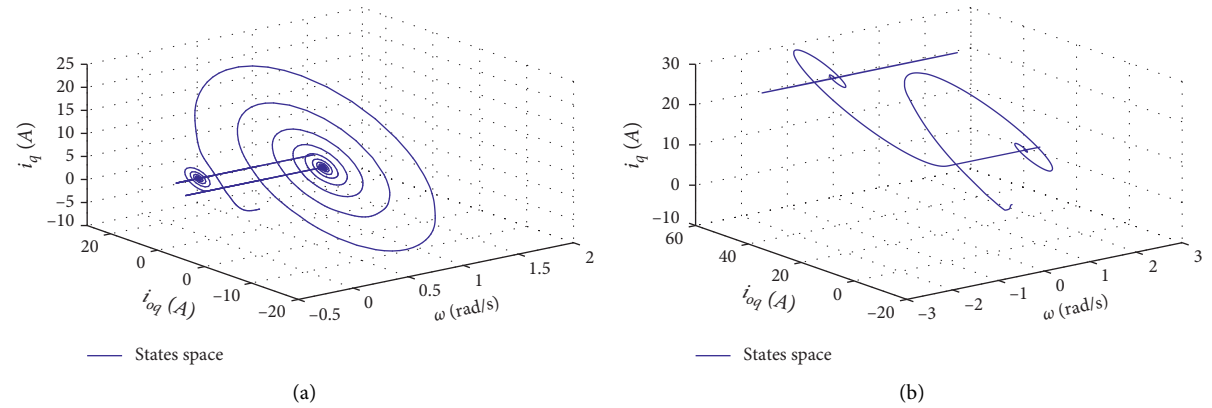

Figure 6: (a) ω, i_{oq}, i_q for BLFs-based CFC. (b) ω, i_{oq}, i_q for DSC.

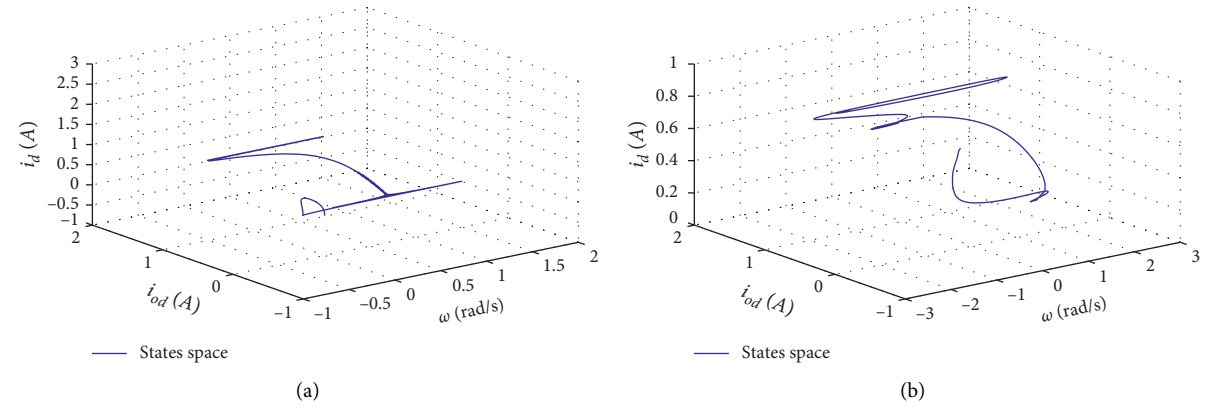

Figure 7: (a) ω, i_{od}, i_d for BLFs-based CFC. (b) ω, i_{od}, i_d for DSC.

developed the BLFs-based adaptive command filtered neural control approach. This approach can not only guarantee that the state variables would confine into reasonable bounds but also ensure that the tracing deviation would congest into a smaller range of zero, which will be much more functional and robust in real-world applications.

Table 2: The comparison performances between CFC and DSC.

Item	CFC	DSC
Absolute percentage of tracking error (%)	0.05	0.2
Variation range of ω	[−0.5, 2]	[−3, 3]
Variation range of i_q	[−10, 25]	[−10, 30]
Variation range of i_{oq}	[−20, 20]	[−20, 60]
Variation range of i_d	[−1, 3]	[0, 1]
Variation range of i_{od}	[−1, 2]	[−1, 2]

7. Conclusion

This paper developed a BLFs-based self-adaptive command filtered neural network control approach to work out the position tracking problem of the PMSM driving system with core losses and all-state restrictions. By merging BLFs into CFC techniques, the issues of "explosion of complexity" and all-state restrictions can be well resolved. Additionally, virtual control laws were constructed to ensure the position tracking error would be limited to a minute range of zero. In the end, simulation performances illustrated the system's adaptability and antidisturbance ability.

Data Availability

The data used to support the findings of this study are partially included within the article. Further information is available from the corresponding author upon request.

Conflicts of Interest

The authors declare that there are no conflicts of interest regarding the publication of this paper.

Acknowledgments

This article was partially supported by the National Key Research and Development Plan (2017YFB1303503), the NSFC (61973179), and the Taishan Scholar Special Project Fund (TSQN20161026).

References

[1] J. K. Seok, J. K. Lee, and D. C. Lee, "Sensorless speed control of nonsalient permanent-magnet synchronous motor using rotor-position-tracking PI controller," *IEEE Transactions on Industrial Electronics*, vol. 53, no. 2, pp. 399–405, 2006.

[2] M. Tursini, F. Parasiliti, and D. Q. Zhang, "Real-time gain tuning of PI controllers for high-performance PMSM drives," *IEEE Transactions on Industry Applications*, vol. 38, no. 4, pp. 1018–1026, 2002.

[3] V. Q. Leu, H. H. Choi, and J.-W. Jung, "Fuzzy sliding mode speed controller for PM synchronous motors with a load torque observer," *IEEE Transactions on Power Electronics*, vol. 27, no. 3, pp. 1530–1539, 2012.

[4] H. Li, P. Shi, D. Yao, and L. Wu, "Observer-based adaptive sliding mode control for nonlinear Markovian jump systems," *Automatica*, vol. 64, pp. 133–142, 2016.

[5] H. L. Liu, X. P. Shi, X. T. Bi, and J. Zhang, "Backstepping based terminal sliding mode control for rendezvous and docking with a tumbling spacecraft," *International Journal of Innovative Computing, Information and Control*, vol. 12, no. 3, pp. 929–940, 2016.

[6] J. Yu, P. Shi, C. Lin, and H. Yu, "Adaptive neural command filtering control for nonlinear MIMO systems with saturation input and unknown control direction," *IEEE Transactions on Cybernetics*, vol. 50, no. 6, pp. 2536–2545, 2020.

[7] Z. Wu, B. Jiang, and Y. Kao, "Finite-time H_∞ filtering for Itô stochastic Markovian jump systems with distributed time-varying delays based on optimisation algorithm," *IET Control Theory & Applications*, vol. 13, no. 5, pp. 702–710, 2019.

[8] H. S. Yu, J. P. Yu, J. Liu, and Q. Song, "Nonlinear control of induction motors based on state error PCH and energy-shaping principle," *Nonlinear Dynamics*, vol. 72, no. 1-2, pp. 49–59, 2013.

[9] C. Fu, Q.-G. Wang, J. Yu, and C. Lin, "Neural network-based finite-time command filtering control for switched nonlinear systems with backlash-like hysteresis," *IEEE Transactions on Neural Networks and Learning Systems*, pp. 1–6, 2020.

[10] W. He, Y. Chen, and Z. Yin, "Adaptive neural network control of an uncertain robot with full-state constraints," *IEEE Transactions on Cybernetics*, vol. 46, no. 3, pp. 620–629, 2016.

[11] J. Yu, P. Shi, J. Liu, and C. Lin, "Neuroadaptive finite-time control for nonlinear MIMO systems with input constraint," *IEEE Transactions on Cybernetics*, pp. 1–8, 2020.

[12] W. J. Dong, J. A. Farrell, M. Polycarpou, V. Djapic, and M. Sharma, "Command filtered adaptive backstepping," *IEEE Transactions on Control Systems Technology*, vol. 20, no. 3, pp. 566–580, 2012.

[13] J. A. Farrell, M. Polycarpou, M. Sharma, and W. Wenjie Dong, "Command filtered backstepping," *IEEE Transactions on Automatic Control*, vol. 54, no. 6, pp. 1391–1395, 2009.

[14] J. P. Yu, P. Shi, X. K. Chen, and G. Z. Cui, "Finite-time command filtered adaptive control for nonlinear systems via immersion and invariance," *SCIENCE CHINA Information Sciences*, 2009.

[15] K. P. Tee, S. S. Ge, and E. H. Tay, "Barrier Lyapunov functions for the control of output-constrained nonlinear systems," *Automatica*, vol. 45, no. 4, pp. 918–927, 2009.

[16] C. Fu, J. Yu, L. Zhao, H. Yu, C. Lin, and Y. Ma, "Barrier Lyapunov function-based adaptive fuzzy control for induction motors with iron losses and full state constraints," *Neurocomputing*, vol. 287, pp. 208–220, 2018.

[17] Y. Liu, J. Yu, H. Yu, C. Lin, and L. Zhao, "Barrier Lyapunov functions-based adaptive neural control for permanent magnet synchronous motors with full-state constraints," *IEEE Access*, vol. 5, pp. 10382–10389, 2017.

[18] X. Yang, J. Yu, Q.-G. Wang, L. Zhao, H. Yu, and C. Lin, "Adaptive fuzzy finite-time command filtered tracking control for permanent magnet synchronous motors," *Neurocomputing*, vol. 337, no. 14, pp. 110–119, 2019.

[19] H. Luo, J. Yu, C. Lin, Z. Liu, L. Zhao, and Y. Ma, "Finite-time dynamic surface control for induction motors with input saturation in electric vehicle drive systems," *Neurocomputing*, vol. 369, no. 5, pp. 166–175, 2019.

[20] J. P. Yu, B. Chen, H. S. Yu, and J. W. Gao, "Adaptive fuzzy backstepping position tracking control for permanent magnet synchronous motor," *Control and Decision*, vol. 25, no. 10, pp. 1547–1551, 2010.

[21] S. Zheng, X. Tang, B. Song, S. Lu, and B. Ye, "Stable adaptive PI control for permanent magnet synchronous motor drive based on improved JITL technique," *ISA Transactions*, vol. 52, no. 4, pp. 539–549, 2013.

[22] H. Li, J. Yu, C. Hilton, and H. Liu, "Adaptive sliding-mode control for nonlinear active suspension vehicle systems using

T-S fuzzy approach," *IEEE Transactions on Industrial Electronics*, vol. 60, no. 8, pp. 3328–3338, 2013.

[23] Q. Yin, M. Wang, and H. Jing, "Stabilizing backstepping controller design for arbitrarily switched complex nonlinear system," *Applied Mathematics and Computation*, vol. 369, Article ID 124789, 2020.

[24] Y. Zhang, C. M. Akujuobi, W. H. Ali, C. L. Tolliver, and L.-S. Shieh, "Load disturbance resistance speed controller design for PMSM," *IEEE Transactions on Industrial Electronics*, vol. 53, no. 4, pp. 1198–1208, 2006.

[25] W. Chang and S. Tong, "Adaptive fuzzy tracking control design for permanent magnet synchronous motors with output constraint," *Nonlinear Dynamics*, vol. 87, no. 1, pp. 291–302, 2017.

[26] G. Cui, J. Yu, and P. Shi, "Observer-based finite-time adaptive fuzzy control with prescribed performance for nonstrict-feedback nonlinear systems," *IEEE Transactions on Fuzzy Systems*, p. 1, 2021.

[27] Y. Wei, J. Qiu, P. Shi, and L. Wu, "A piecewise-Markovian Lyapunov approach to reliable output feedback control for fuzzy-affine systems with time-delays and actuator faults," *IEEE Transactions on Cybernetics*, vol. 48, no. 9, pp. 2723–2735, 2018.

[28] Z. Zhao, J. Yu, L. Zhao, H. Yu, and C. Lin, "Adaptive fuzzy control for induction motors stochastic nonlinear systems with input saturation based on command filtering," *Information Sciences*, vol. 463-464, pp. 186–195, 2018.

[29] Z. Y. Cui, R. M. Ke, and Y. H. Wang, "Deep bidirectional and unidirectional LSTM recurrent neural network for network-wide traffic speed prediction," 2018, https://arxiv.org/abs/1801.02143.

[30] X.-B. Jin, H.-X. Wang, X.-Y. Wang, Y.-T. Bai, T.-L. Su, and J.-L. Kong, "Deep-Learning prediction model with serial two-level decomposition based on bayesian optimization," *Complexity*, vol. 2020, Article ID 4346803, 14 pages, 2020.

[31] R. Fu, Z. Zhang, and L. Li, "Using LSTM and GRU neural network methods for traffic flow prediction," in *Proceedings of the 2016 31st Youth Academic Annual Conference of Chinese Association of Automation (YAC)*, pp. 324–328, Wuhan, China, November 2016.

[32] Y. T. Bai, X. B. Jin, X. Y. Wang, T. L. Su, J. L. Kong, and Y. T. Lu, "Compound autoregressive network for prediction of multivariate time series," *Complexity*, vol. 2019, Article ID 9107167, 11 pages, 2019.

[33] X. B. Jin, C. Dou, T. L. Su, X. F. Lian, and Y. Shi, "Parallel irregular fusion estimation based on nonlinear filter for indoor RFID tracking system," *International Journal of Distributed Sensor Networks*, vol. 2016, no. 8, Article ID 1472930, 11 pages, 2016.

[34] Y.-T. Bai, X.-Y. Wang, X.-B. Jin, Z.-Y. Zhao, and B.-H. Zhang, "A neuron-based Kalman filter with nonlinear autoregressive model," *Sensors*, vol. 20, no. 1, p. 299, 2020.

[35] M. Chen, G. Tao, and B. Jiang, "Dynamic surface control using neural networks for a class of uncertain nonlinear systems with input saturation," *IEEE Transactions on Neural Networks and Learning Systems*, vol. 26, no. 9, pp. 2086–2097, 2015.

[36] J. Ma, Z. Zheng, and P. Li, "Adaptive dynamic surface control of a class of nonlinear systems with unknown direction control gains and input saturation," *IEEE Transactions on Cybernetics*, vol. 45, no. 4, pp. 728–741, 2015.

[37] Y. Bai, X. Wang, X. Jin, T. Su, J. Kong, and B. Zhang, "Adaptive filtering for MEMS gyroscope with dynamic noise model," *ISA Transactions*, vol. 101, pp. 430–441, 2020.

[38] X. Zhang, F. Ding, L. Xu, and E. Yang, "State filtering-based least squares parameter estimation for bilinear systems using the hierarchical identification principle," *IET Control Theory & Applications*, vol. 12, no. 12, pp. 1704–1713, 2018.

[39] X. Zhang, F. Ding, L. Xu, and E. Yang, "Highly computationally efficient state filter based on the delta operator," *International Journal of Adaptive Control and Signal Processing*, vol. 33, no. 6, pp. 875–889, 2019.

[40] Y.-J. Liu, J. Li, S. Tong, and C. L. P. Chen, "Neural network control-based adaptive learning design for nonlinear systems with full-state constraints," *IEEE Transactions on Neural Networks and Learning Systems*, vol. 27, no. 7, pp. 1562–1571, 2016.

[41] J. Yu, L. Zhao, H. Yu, and C. Lin, "Barrier Lyapunov functions-based command filtered output feedback control for full-state constrained nonlinear systems," *Automatica*, vol. 105, pp. 71–79, 2019.

[42] Z. Zhao, X. Wang, P. Yao, and Y. Bai, "A health performance evaluation method of multirotors under wind turbulence," *Nonlinear Dynamics*, vol. 102, no. 3, pp. 1701–1715, 2020.

[43] F. Ding, L. Xu, D. D. Meng, X. B. Jin, A. Alsaedi, and T. Hayate, "Gradient estimation algorithms for the parameter identification of bilinear systems using the auxiliary model," *Journal of Computational and Applied Mathematics*, vol. 369, Article ID 112575, 2019.

[44] F. Ding, L. Lv, J. Pan, X. Wan, and X.-B. Jin, "Two-stage gradient-based iterative estimation methods for controlled autoregressive systems using the measurement data," *International Journal of Control, Automation and Systems*, vol. 18, no. 4, pp. 886–896, 2020.

[45] X. Zhang, F. Ding, and L. Xu, "Recursive parameter estimation methods and convergence analysis for a special class of nonlinear systems," *International Journal of Robust and Nonlinear Control*, vol. 30, no. 4, pp. 1373–1393, 2020.

[46] J. Yu, P. Shi, W. Dong, B. Chen, and C. Lin, "Neural network-based adaptive dynamic surface control for permanent magnet synchronous motors," *IEEE Transactions on Neural Networks and Learning Systems*, vol. 26, no. 3, pp. 640–645, 2015.

[47] Y.-J. Liu and S. Tong, "Adaptive NN tracking control of uncertain nonlinear discrete-time systems with nonaffine dead-zone input," *IEEE Transactions on Cybernetics*, vol. 45, no. 3, pp. 497–505, 2015.

[48] B. B. Ren, S. Z. Ge, and K. P. Tee, "Adaptive neural control for output feedback nonlinear systems using a Barrier Lyapunov function," *IEEE Transactions on Neural Networks and Learning Systems*, vol. 21, no. 8, pp. 1339–1345, 2010.